# Archaeomagnetic Study of Roman Lime Kilns (1st c. AD) and One Pottery Kiln (1st c. BC – 1st c. AD) at Krivina, Bulgaria, as a Contribution to Archaeomagnetic Dating

ARCHAEOLOGIA BULGARICA
XIV, 2 (2010), 23-38

**Fabio DONADINI / Mary KOVACHEVA / Maria KOSTADINOVA-AVRAMOVA**

**ABSTRACT**

We present a detailed archaeomagnetic study of the remains of seven lime kilns and one pottery kiln discovered at the Danube bank in North Eastern Bulgaria. These kilns belong to four structures according to their spatial distribution, and relate to the beginning of our era. The collection of samples shows favourable rock magnetic properties, ensuring reliable archaeomagnetic measurements. In this work we studied both directions (Declination D, Inclination I) and intensity (Ba) of the geomagnetic field at the time of the last use of the kilns. These results can be used as reference points for ameliorating the Bulgarian palaeosecular archaeomagnetic curves as well as for global and regional geomagnetic field models, which can be in turn used for archaeomagnetic dating.

Part of the collection was studied at the Scripps Institution of Oceanography in San Diego, and part at the Palaeomagnetic laboratory of the Geophysical Institute of the Bulgarian Academy of Sciences (Sofia). The excellent agreement between these independent measurements indicates the high quality of the material and the validity of the methods applied.

The results are summarized as structure averages, which represent units of kilns. Structure 1 to 3 are assumed to be contemporaneous, and yield D: 353.6°, I: 60.7°, Ba: 67.2 μT (Structure 1), D: 356.2°, I: 56.6°, Ba: 63.2 μT (Structure 2), D: 356.5°, I: 57.4°, Ba: 67.9 μT (Structure 3 – the big twin kilns). Structure 4 appears older based on archaeological evidences, and produces D: 359.9°, I: 67.6°, Ba: 69.0 μT. Statistical test to compare the average directions from the four structures also reject the hypothesis for a common mean between structure 4 and the others at 95% confidence interval. This indicates that the time when structure 4 (pottery kiln) was last used differs from the time when the other structures were fired.

These new results partly fill up one of the gaps (150 BC to 85 AD) in the Bulgarian master curves, and show that improvements of ancient geomagnetic field modelling can be achieved only with new archaeomagnetic studies of well dated collections.

**INTRODUCTION**

The geomagnetic field slightly changes its pole position during the centuries, as well as its intensity. These changes are tied to processes occurring in the outer core of the Earth, and can be described by moving non dipolar parts of the geomagnetic field (Merrill et al. 1996).

From a global perspective, it is possible to model the geomagnetic field changes using spherical harmonics, and the accuracy of these models is proportional to the amount and the distribution of measurements available.

Direct measurements from magnetic observatories cover in detail the past 3 to 4 centuries, and so archaeological artefacts represent the main source of measurements to constrain the geomagnetic field evolution before this time.

At a regional level, the employment of master curves (e.g. Donadini et al. 2009, for a review) or other spherical (cap) harmonic models (Lodge and Holme 2008; Pavon-Carrasco et al. 2008 and 2009) to date archaeological sites has become a widely used technique. Its accuracy can be pretty high.

In particular, various master curves constructed with data from a particular region are available (Kovacheva et al. 1998; LeGoff et al. 2002; Tema et al. 2006; Gomez-Paccard et al. 2006; Schnepp / Lanos, 2006; Marton 2010). The Bulgarian one is at present one of the most detailed ones, and consists of about 320 independent directional and/or intensity studies covering the longest interval of time (the last 8000 years). Despite that, there are still gaps in this database, and one of these appears between 150 BC and 85 AD. The Krivina kilns are archaeologically around the beginning of our era, and they represent time intervals where there are very few data in Bulgaria. Including new data for this period will increase the accuracy of the local master curve used for dating purposes.

## MATERIAL STUDIED

The material is represented by well baked to partly vitrified clay from the walls of seven remnants of lime kilns belonging to the *Legio I Italica* about 2000 years ago, and one earlier pottery kiln. Most kilns were very well preserved; most lime kilns were still intact, whereas only the floor of the pottery kiln was still preserved. More precisely, structures 1 to 3 are archeologically dated at the last third of the 1$^{st}$ century AD, whereas structure 4 has an age of 1$^{st}$ century BC to beginning of the 1$^{st}$ century AD (Vagalinski in press a, b). For this study we transformed the dates in absolute age intervals: 70 to 100 AD for structures 1 to 3, and 60 BC to 30 AD for structure 4. This dating relies on the archaeological context (well known presence of the Roman Legion at that time) as well as on the stratigraphic information (Structure 4 comes from a lower horizon compared to the other structures). The kilns are located near the village of Krivina, Svishtov district in North Bulgaria, at 43.64°N and 25.59°E.

In total, 59 oriented hand samples (**fig. 1**) were collected from the four structures. Orientation marks were done using both a magnetic and a sun compass on a horizontal plaster of Paris surface. The samples were well baked and consolidated, so they could be directly cut into specimens without problems. In general, 3 to 10 specimens were obtained from each sample depending on its size.

## MEASUREMENTS PERFORMED

Part of the measurements was carried out at the Scripps Institution of Oceanography in San Diego, and part at the Bulgarian Academy of Sciences in Sofia, using slightly different methods and equipments. By this way, we obtain independent measurements that allow a cross-validation of the results.

The baked archaeological clay carries a ThermoRemanent Magnetization (TRM), which gives the possibility to recover the geomagnetic field elements (Declination, Inclination, and Intensity) for the date and place of its last heating.

Rock magnetic measurements aiming to define the magnetic carriers composing the clays, as well as to check the level of alteration of the minerals while

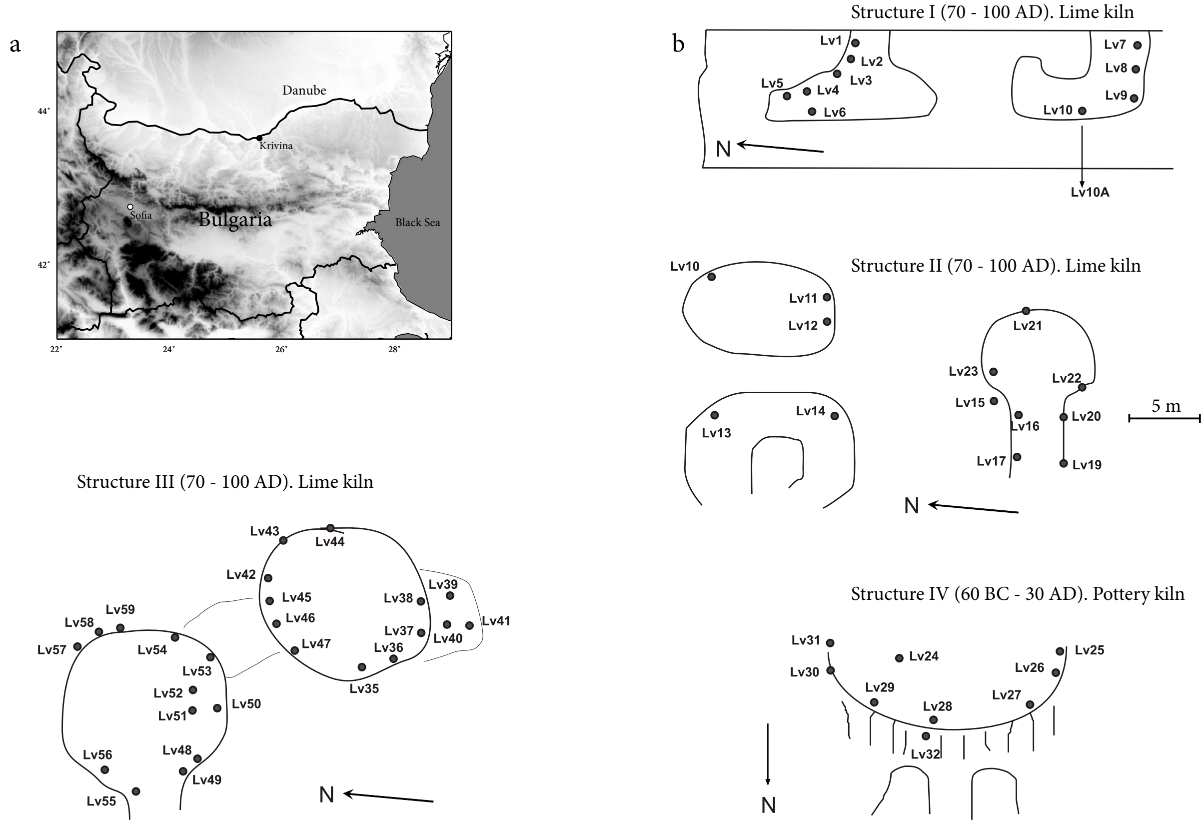


**Fig. 1: a** – Location of the Roman kilns at Krivina displayed on a DEM map of Bulgaria using GMT (Wessel / Smith 1991); **b** – distribution of samples from the different structures.

heating, consisted of high temperature susceptibilities, hysteresis cycles, thermal demagnetization (Lowrie 1990) of three axes laboratory imparted Isothermal Remanent Magnetization (IRMs), thermal demagnetization of Saturated Isothermal Remanent Magnetization (SIRM), with re-saturation at each thermal step (Jordanova et al. 1997), Lowrie-Fuller (1971) test (L-F), and viscous tests.

Archaeomagnetic and archaeointensity determinations were carried out with a good knowledge of the magnetic mineralogy. Magnetic directions were determined as a mixture of alternating field, thermal demagnetizations, and viscous cleaning of the specimens.

To obtain the final directions (declination D and inclination I) for each structure we adopt the hierarchical approach (e.g. Lanos et al. 2005) where first samples averages are considered and then structure ones. To define the scatter of direction we adopt Fisher statistics (Fisher 1953), which includes the precision parameter K and the $\alpha_{95}$. The K describes the dispersion between individual results, and it is high when results are well clustered. The $\alpha_{95}$ is the semi angle of the cone of confidence for the calculated average direction. Small values of $\alpha_{95}$ correspond to a best defined average direction.

Intensities were determined using the IZZI protocol (Tauxe / Staudigel 2004) at Scripps, or using the Coe (1967) protocol at Sofia. Average intensities are calculated at a structure level using weighted statistics (Kovacheva / Kanarchev 1986). The results are given as average and 1 standard deviation. To identify suitable results, we determine the Difference Ratio Sum (DRATS; Tauxe et al. 2009), which indicates the percentage of change in magnetic acquisition after heating the specimen at a higher temperature. In this case a small percentage of change is indicative for reliable samples. We also define the f fraction (Coe 1967), which represents the percentage of magnetization used to define the paleointensity. The larger

| | Sample | Sv [%] | Kfd [%] | MDF [mT] | L-F test | 3-IRM test | | | High Temp Susc. | | SIRM test | Hc [mT] | Hcr [mT] | Mrs [emu/g] | Ms [emu/g] | Loop Type |
|---|---|---|---|---|---|---|---|---|---|---|---|---|---|---|---|---|
| | | | | | | soft Tdb [˚C] | intermediate Tdb [˚C] | hard Tdb [˚C] | Curie Temper. Tc [˚C] | Alteration | | | | | | |
| Struct. 1 | LV01 | 7 | 9 | 20 | 0.09 / SD | 540; 620 | - | 700 | | | Positive | 7.45 | 16.18 | 40.50 | 204.30 | |
| | LV05 | 7 | 13 | 18 | 0.28 / BM | | | | | | | | | | | |
| | LV08 | 9 | 7 | 25 | 0.13 / SD | 540 | - | 160; 700 | | | | 5.87 | 22.53 | 54.04 | 389.00 | |
| Struct. 2 | LV11 | 6 | 8 | | | | | | | | | 7.64 | 17.14 | 25.32 | 142.60 | |
| | LV12 | 6 | 6 | too hard | infinite | 300; 580 | 180; 700 | 250; 580; 700 | | | Positive | | | | | |
| | LV13 | | | | | | | | 480; 567 | high | | 10.48 | 23.01 | 28.55 | 147.70 | |
| | LV14 | 10 | 6 | 18 | 0.22 / SD | 620 | - | - | | | Positive | | | | | |
| | LV15 | 12 | 9 | | | | | | | | | 10.57 | 35.83 | 4.29 | 26.77 | |
| | LV16 | 9 | 9 | 25 | infinite | 540; 700 | 700 | 240; 700 | | | Positive | | | | | |
| | LV19 | 10 | 9 | | | | | | 569 | none | | 16.14 | 83.71 | 6.16 | 24.18 | WW |
| Struct. 4 | LV24 | 8 | 8 | 14,5 | -0.48 / MD | 540 | 250 | 250 | | | Positive | | | | | |
| | LV26 | 10 | 5 | 15 | 0.51 / BM | 540; 620 | - | - | 580 | none | Positive | 9.68 | 19.65 | 25.48 | 126.40 | |
| | LV27 | | | | | | | | 595 | | | 9.09 | 19.80 | 9.26 | 54.33 | |
| | LV29 | 6 | 7 | 25 | | | | | 272; 595 | moderate | | 7.89 | 17.25 | 51.80 | 282.30 | |
| | LV31 | 3 | 9 | 19 | 0.34 / BM | | | | | | | | | | | |
| Struct. 3 | LV35 | 5 | | | | | | | 540 | moderate | | 7.85 | 23.43 | 17.10 | 90.71 | WW |
| | LV37 | 7 | | 14,5 | 0.21 / SD, MX | 540 | - | - | 520 | moderate | Positive | 9.73 | 18.70 | 34.20 | 118.80 | |
| | LV41 | 13 | | 25 | 0.35 / SD | 540; 620 | 160; 700 | 250; 620; 700 | | | | 10.17 | 37.53 | 2.49 | 13.87 | WW |
| | LV43 | 4 | 7 | 14 | 0.28 / BM | 580 | - | - | | | Positive | | | | | |
| | LV50 | 7 | 7 | 15 | 0.31 / BM | 540; 620 | - | - | | | Positive | | | | | |
| | LV51 | 12 | 10 | | | | | | | | | 7.82 | 19.86 | 43.73 | 236.50 | |
| | LV52 | 14 | 10 | 28 | 0.28 / BM | 540 | - | - | | | Positive | | | | | |
| | LV56 | 10 | 11 | | | 620 | 700 | 480; 700 | | | | | | | | |
| | LV57 | 18 | 8 | | | | | | | | | 13.91 | 36.58 | 12.92 | 49.71 | |

**Table 1.** Rock magnetic results for various specimens of the Kilns.

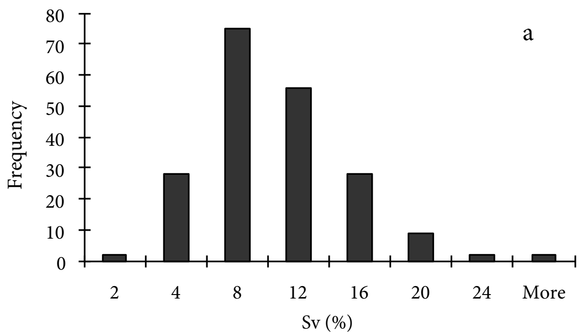


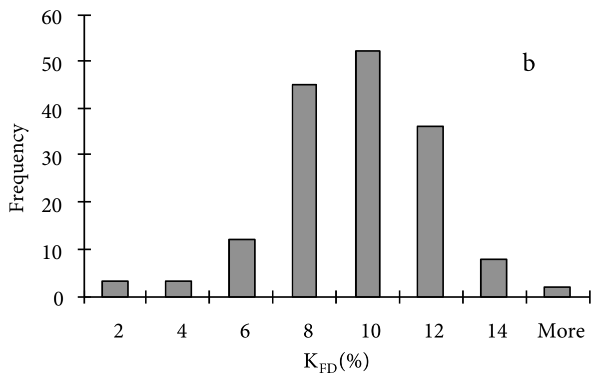


**Fig. 2: a** – Histogram of the viscous coefficient Sv; **b** – Histogram of the frequency dependent magnetic susceptibility Kfd (Dunlop / Ozdemir 1997).

part of magnetization taken into account, the more reliable is the result. To quantify the influence of non ideal grains, the Natural Remanent Magnetization (NRM) measurements can be repeated after a Partial ThermoRemanent Magnetization (pTRM) is imparted at a certain temperature. In this case we perform a tail check (Riisager / Riisager 2001), where we monitor the change in NRM; a small change is indicative of well behaving samples.

## ROCK MAGNETIC RESULTS

Our rock magnetic investigations indicate that the material is highly suitable for archaeomagnetic studies. The main results of the various tests are summarized in **table 1**. Viscous magnetization lost during three weeks of sample storage in zero field, inside mu-metal shields, is about 8-12% (**fig. 2a**). **Figure 2b** shows the frequency dependent susceptibility (Kfd) histogram, and indicates large contribution of very fine superparamagnetic (SP) grains. Most likely, the large amount of SP grains is also responsible for the rather large Sv values. These very fine particles originate in antiquity during heating in oxidizing conditions, e.g. from the exterior of the walls (Herries / Kovacheva 2007). Specimens from the inner vitrified part of the kiln wall (**fig. 3b,c**) were formed under reductive conditions and have less contribution of SP grains (e.g. sample LV23 has lowest Kfd values). Samples formed in reducing conditions have generally grey-black colour, whereas oxidized ones are red-orange. For our paleointensity analyses we discarded samples that have viscous coefficients (Sv) larger than 8%.

Lowrie-Fuller test (Lowrie / Fuller 1971) was performed on 14 selected specimens from the four structures. Grain size distinction based on Dunlop (1983) classification indicates a mixture of bimodal (i.e. both fine and coarse grains) as well as only single domain carriers. This is consistent with the hysteresis parameters measured on 14 specimens, which in general show that samples lie at the MD-SD mixing line (Dunlop 2002) boundary on the Day plot (**fig. 4a**). Exceptions are represented by samples that present more or less pronounced wasp-waisted loops. Hysteresis loops show that saturation is reached in general at about 300 μT, indicative for magnetite as a carrier (**fig. 4b**). In few cases, the loop does not close up to 1T, showing the presence of other hard magnetic phases (**fig. 4c**).

High temperature susceptibilities were measured on 7 specimens (**table 1**, **fig. 5**). In general, (titano)magnetite was detected as a main magnetic carrier (Curie Temperature around 540-580°C). This is in agreement with the Median Destructive Field (MDF, **table 1**, column 5) obtained by the L-F test. The most important observation from these experiments is that only minor thermochemical changes appear during heating. Only sample LV13 shows a sharp increase of susceptibility on the cooling curve, which may be attributed to hematite reduction into magnetite. This sample was excluded from further analyses.

Three-axes IRM tests (Lowrie 1990) were also performed on 13 specimens. In all specimens soft magnetic component is the prevailing carrier and it is associated with low titanium magnetite (Tc at about 540°C). Specimen LV12 shows an additional soft component with Tc around 300°C which can be attributed to maghemite.

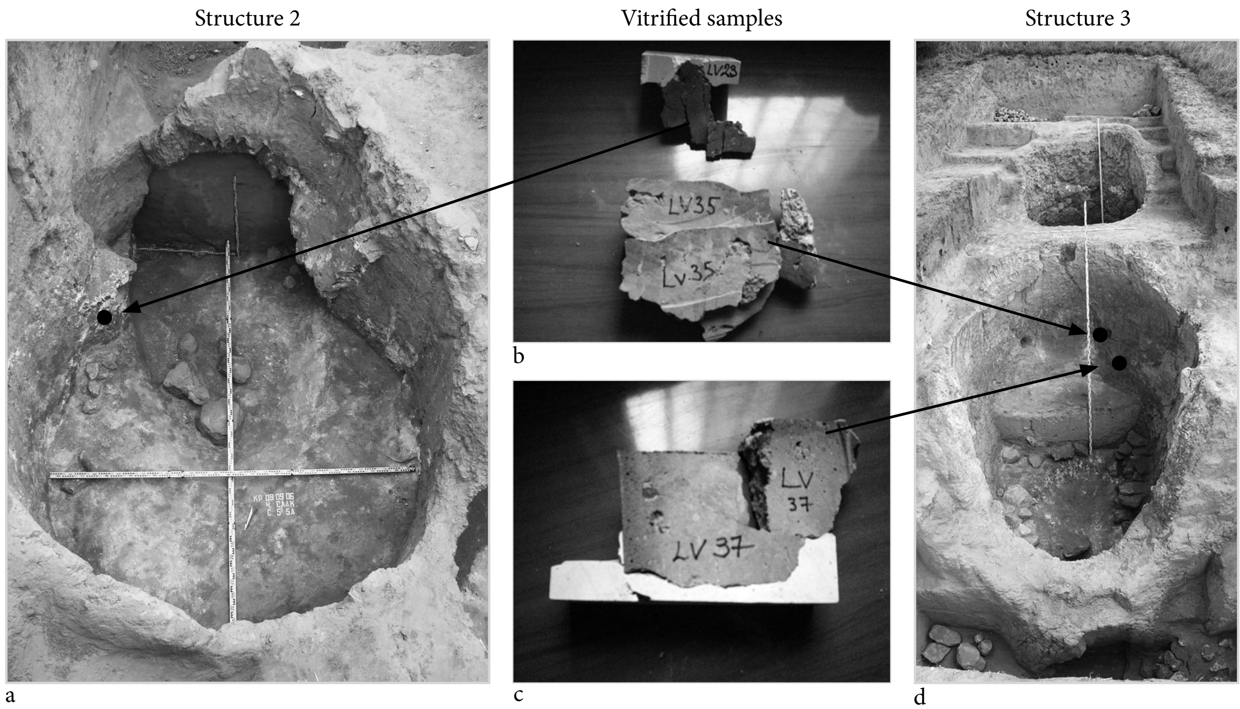


**Fig. 3**: **a**, **d** – Photo of Lime kiln number 2 and 3, respectively; **b, c** – Photos of the vitrified samples from the inside of the furnaces. Photos of the two structures provided by L. Vagalinski.

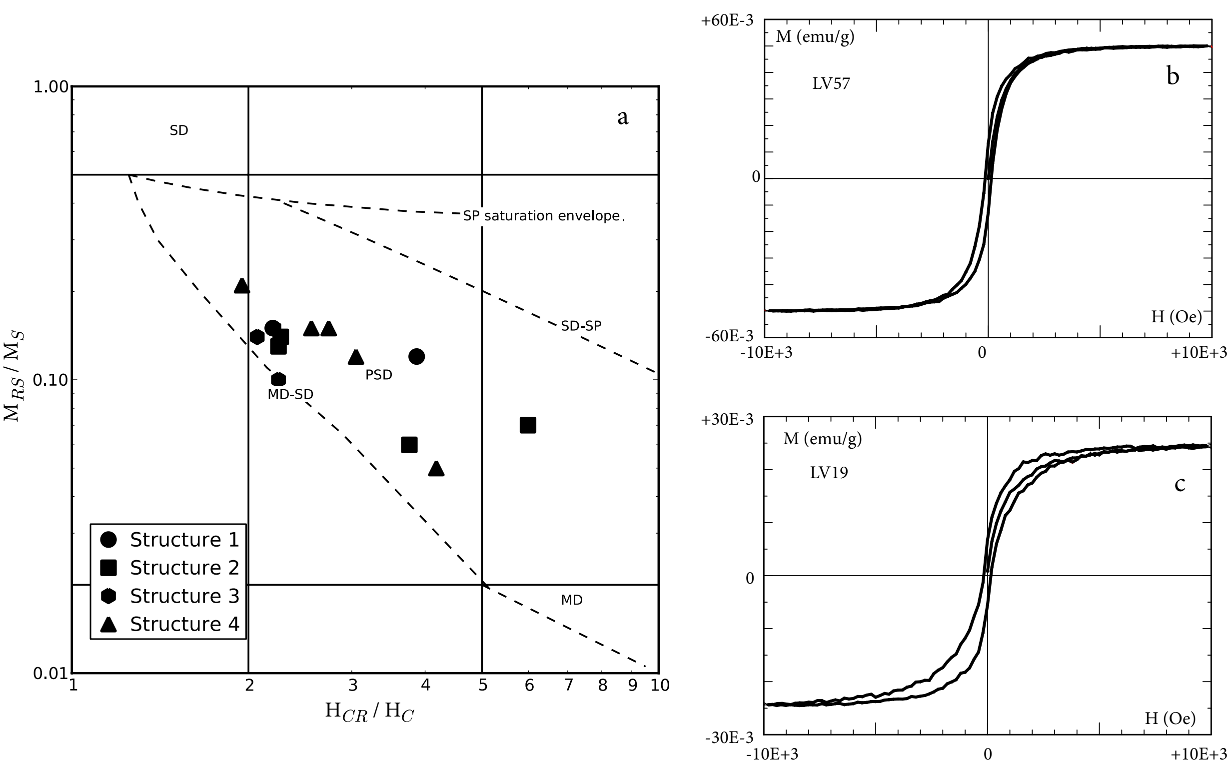


**Fig. 4**: **a** – Day plot indicating the values of samples from the four structures; **b**, **c** – Typical hysteresis loops obtained from the Krivina samples.

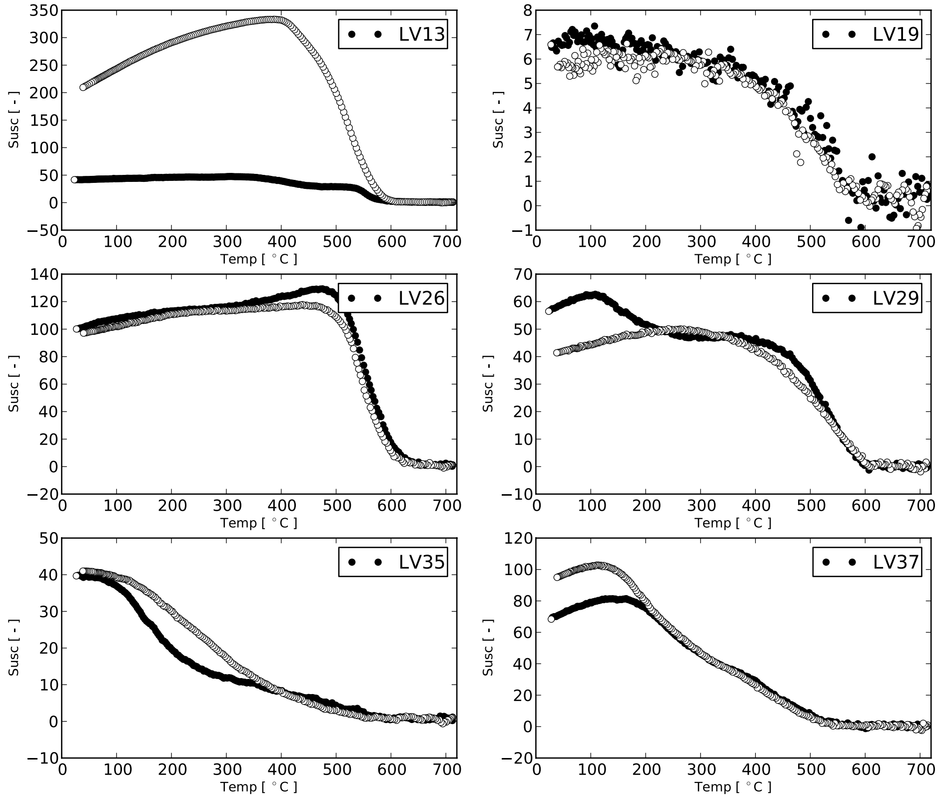


**Fig. 5.** High temperature susceptibility curves for six analysed samples. Heating (cooling) curve denoted by closed (empty) circles.

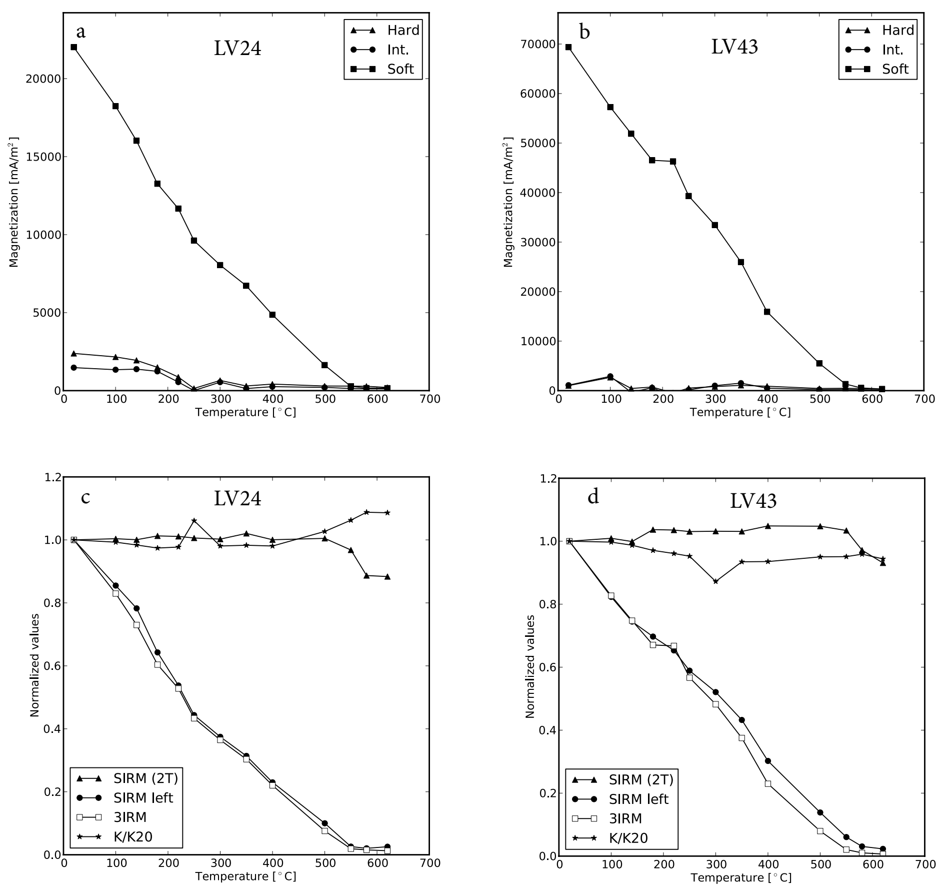


**Fig. 6**: **a**, **b** – Three-axes IRM experiments for samples LV24 and LV43, respectively. LV24 has soft components Tc around 580˚C corresponding to magnetite, as well as Tc for small hard and medium components at around 250˚C; **c, d** – SIRM tests for the same samples. In both cases no alteration while heating is observed, indicating good thermal stability of the magnetic phases.

Hard components are detected in quite some specimens, although there might not be an evidence of it in the hysteresis loops from sister specimens. This is especially true when the soft magnetic component is dominant compared to the intermediate or the hard one. We observe in many cases hematite (Tc above 680˚C). In most of cases its contribution to the signal is insignificant (**table 1** and **fig. 6a**). In few cases we observe a well expressed hard phase with Tc around 250˚C. This latter might be not yet precisely defined substituted hematite as suggested by McIntosh et al. (2007).

All the SIRMs performed (10 specimens) indicate that no mineralogical change occurs while heating, and so all tests are positive (**table 1**, **fig. 6**). This behaviour is a prerequisite for reliable paleointensity experiments, which involve several heating steps at various temperatures (Jordanova et al. 2003).

In summary, the rock magnetic analyses indicate that the main carrier is associated with (titano)magnetite. Based on 3IRM tests, samples LV12, LV16 and LV41 contain greatest or considerable concentrations of magnetically hard components. This observation is backed up in case of LV41 by its wasp-waisted hysteresis loop. Sample LV19 shows a very pronounced wasp-waisted loop; however no 3IRM test was made on this sample, but viscosity and Kfd tests point to considerable SP fraction. In the case of the next observed wasp-waisted loop (LV37 – **table 1**) the studied material obviously is taken from the orange outer part of the hand sample with a developed considerable fraction of SP grains (3IRM test has not shown any hard magnetically component).

Both SIRM tests and high temperature susceptibility experiments are consistent with each other and point to minor to no mineralogical changes during heating. This stable behaviour is one of the main prerequisites for reliable archaeomagnetic investigations.

The carbon released during lime production ensures reducing conditions in the inside of the kiln, and leads to formation of brownish-gray, vitrified parts. The outside of the kiln lies in an oxidizing atmosphere, and so the colour of the clays becomes more orange-red. Our rock magnetic analyses support this evidence: samples from the reducing side (e.g. LV35 and LV37) have Curie temperatures of 540˚-580˚C, typical for magnetite, small Sv coefficients (i.e. less SP grains), and do not show evidences of hard magnetic phases as hematite (e.g. from 3IRM test).

## DIRECTIONAL RESULTS

Directional data are obtained from oriented hand samples that are collected in situ. These hand samples are then cut in the laboratory in many cubic subsamples (specimens) that fit the magnetometer. These procedures might sometimes produce errors: for example, if the sample is badly oriented in the field, or if the cutting into subsamples is difficult, as in the case of fragile samples. In our analysis we had to reject some of the results where an operator mistake was obvious. In total, the results of six specimens were rejected for these reasons. Similarly, if the average of a sample yields directions that are clearly inconsistent with the ones of other samples in the same structure, then these are also rejected (here sample LV23, Structure 2, marked with ** in **table 2**).

**Table 2** gives the directional results at sample level for all structures, including statistics. There are only 3 cases for which only one specimen was cut (LV49, LV57, and LV58), and so no statistical evaluation was possible.

At a sample level, results were accepted in case the average of the specimens has a $\alpha_{95}$<6˚, and so sample LV26 was rejected (marked with * in **table 2**).

| | Sample | D [°] | Dcont | Dcorr [°] | I [°] | n | R | K | $\alpha_{95}$ [°] |
|---|---|---|---|---|---|---|---|---|---|
| Structure 1 | LV01 | 347.4 | 5.7 | 353.1 | 62.3 | 6 | 5.999 | 3891.9 | 1.1 |
| | LV02 | 345.8 | 5.7 | 351.5 | 63.4 | 7 | 6.974 | 231.6 | 4.0 |
| | LV03 | 351.6 | 5.7 | 357.3 | 60.9 | 4 | 3.991 | 314.8 | 5.2 |
| | LV04 | 334.1 | 5.7 | 339.8 | 63.8 | 8 | 7.992 | 834 | 1.9 |
| | LV05 | 342.4 | 5.7 | 348.1 | 59.8 | 4 | 3.995 | 570.2 | 3.9 |
| | LV06 | 356.5 | 5.7 | 362.2 | 59.2 | 3 | 3.000 | 4247.9 | 1.9 |
| | LV07 | 352.9 | 5.7 | 358.6 | 57.3 | 5 | 4.999 | 2732 | 1.5 |
| | LV08 | 358.6 | 5.7 | 364.3 | 58.7 | 11 | 10.986 | 732.8 | 1.7 |
| | LV09 | 344.1 | 5.7 | 349.8 | 61.5 | 4 | 3.992 | 394.7 | 4.6 |
| | LV10 | 343.2 | 5.7 | 348.9 | 57.8 | 3 | 2.999 | 2869 | 2.3 |
| | **Mean** | | | **353.6** | **60.7** | **10** | **9.975** | **362.4** | **2.5** |
| Structure 2 | LV11 | 351.8 | 3.6 | 355.4 | 56.9 | 3 | 3.000 | 8163.3 | 1.4 |
| | LV12 | 351.9 | 3.6 | 355.5 | 54.3 | 6 | 5.973 | 183.5 | 5.0 |
| | LV14 | 356.7 | 3.6 | 0.3 | 57.1 | 4 | 3.992 | 373 | 4.8 |
| | LV15 | 352.7 | 3.6 | 356.3 | 52.7 | 3 | 2.998 | 1020.9 | 3.9 |
| | LV16 | 352.1 | 3.6 | 355.7 | 52.2 | 7 | 6.989 | 529.4 | 2.6 |
| | LV17 | 356.9 | 3.6 | 0.5 | 57.5 | 5 | 4.997 | 1269.8 | 2.1 |
| | LV19 | 346.2 | 3.6 | 349.8 | 62.9 | 2 | 2.000 | 3612.4 | 4.2 |
| | LV20 | 351.5 | 3.6 | 355.1 | 59.0 | 10 | 9.989 | 792 | 1.7 |
| | LV23** | 7.4 | 3.6 | 11.0 | 47.9 | 3 | 2.999 | 2062.9 | 2.7 |
| | **Mean** | | | **356.2** | **56.6** | **8** | **7.984** | **425.8** | **2.7** |
| Structure 3 | LV35 | 354.2 | 1.7 | 355.9 | 57.5 | 4 | 3.998 | 1181.1 | 2.7 |
| | LV36 | 348.9 | 1.7 | 350.6 | 56.8 | 2 | 2 | 154202 | 0.7 |
| | LV37 | 351.8 | 1.7 | 353.5 | 57.0 | 5 | 4.995 | 858.1 | 2.6 |
| | LV38 | 350.8 | 1.7 | 352.5 | 60.0 | 8 | 7.971 | 243.5 | 3.6 |
| | LV40 | 351.1 | 1.7 | 352.8 | 58.3 | 4 | 3.997 | 935.7 | 3.0 |
| | LV41 | 343.5 | 1.7 | 345.2 | 62.7 | 5 | 4.988 | 329.6 | 4.2 |
| | LV42 | 349.8 | 1.7 | 351.5 | 56.8 | 8 | 7.995 | 1294.7 | 1.5 |
| | LV43 | 344.8 | 1.7 | 346.5 | 61.8 | 7 | 6.996 | 1602 | 1.5 |
| | LV44 | 349.3 | 1.7 | 351.0 | 57.4 | 4 | 3.998 | 1579.5 | 2.3 |
| | LV45 | 349.8 | 1.7 | 351.5 | 56.0 | 5 | 4.991 | 419.3 | 3.7 |
| | LV46 | 359.9 | 1.7 | 1.6 | 56.7 | 4 | 3.993 | 399.4 | 4.6 |
| | LV47 | 346.3 | 1.7 | 348.0 | 57.0 | 3 | 2.999 | 1866.1 | 2.9 |
| | LV48 | 3.6 | 1.7 | 5.3 | 56.0 | 2 | 2.000 | 2190.6 | 5.3 |
| | LV49 | 2.2 | 1.7 | 3.9 | 55.7 | 1 | | | |
| | LV50 | 358.8 | 1.7 | 0.5 | 54.4 | 10 | 9.977 | 388.1 | 2.5 |
| | LV51 | 6.2 | 1.7 | 7.9 | 52.5 | 4 | 3.995 | 568 | 3.9 |
| | LV52 | 356.1 | 1.7 | 357.8 | 57.6 | 7 | 6.995 | 1268.4 | 1.7 |
| | LV53 | 352.2 | 1.7 | 353.9 | 53.8 | 5 | 4.998 | 1958.9 | 1.7 |
| | LV54 | 350.3 | 1.7 | 352.0 | 58.1 | 5 | 4.996 | 896.1 | 2.6 |
| | LV55 | 6.4 | 1.7 | 8.1 | 50.2 | 4 | 3.997 | 857.6 | 3.1 |
| | LV56 | 14.2 | 1.7 | 15.9 | 59.7 | 3 | 2.999 | 3604.0 | 2.1 |
| | LV57 | 359.7 | 1.7 | 1.4 | 58.2 | 1 | | | |
| | LV58 | 344.2 | 1.7 | 345.9 | 59.4 | 1 | | | |
| | **Mean** | | | **356.5** | **57.4** | **23** | **22.911** | **247.8** | **1.9** |
| Structure 4 | LV24 | 347.7 | 5.9 | 353.6 | 64.2 | 10 | 9.990 | 854.7 | 1.7 |
| | LV26* | 351.5 | 5.9 | 357.4 | 68.5 | 2 | 1.997 | 347.1 | 13.4 |
| | LV29 | 341.1 | 5.9 | 347.0 | 67.8 | 3 | 2.997 | 645.9 | 4.9 |
| | LV30 | 0.5 | 5.9 | 6.4 | 68.1 | 3 | 2.999 | 1550 | 3.1 |
| | LV31 | 6.9 | 5.9 | 12.8 | 62.7 | 9 | 8.996 | 2217.4 | 1.1 |
| | LV32 | 351.6 | 5.9 | 357.5 | 73.6 | 3 | 2.999 | 2027.8 | 2.7 |
| | **Mean** | | | **359.9** | **67.6** | **5** | **4.979** | **190.6** | **5.6** |

**Table 2.** Directional results of samples and averages for each structure. Dcorr is the corrected declination (D) after the sun compass consideration, I is inclination. The number of specimen (n), the vector resultant R (which approaches n when the precision is high), the precision parameter K, and the cone of confidence $\alpha_{95}$ are also given.

All thermal (TH) and alternating field (AF) treatments isolate a single component with little viscous overprint, removed in general at 100˚C or 5-10 μT (Insets of **fig. 7**). For this reason, the results of most of the sub-samples were simply taken using the NRM measured after 3 weeks of storage in zero-field to eliminate the unstable viscous components.

Strongly magnetized bodies like our kilns lead to a deviation of the magnetic orientation which can be corrected using a sun compass. At Krivina it was not possible to get a sun direction for all samples, and so we decided to take an average of all existing sun marks in a corresponding structure to correct the final magnetic declination. Directions are given as raw values (D in **table 2**) and corrected for the average present declination value at the structure (Dcorr in **table 2**).

The accepted samples were averaged to calculate a site mean for each of the structures. The hierarchical approach proves to be better because our results are better clustered, and is in agreement with observations after Lanos et al. (2005). Structures 1 to 3 yield results with good internal consistency defined by the high precision parameters K and small $\alpha_{95}$. Results from structure 4 appear more scattered, and so we get an $\alpha_{95}$ of 5.6˚.

## PALEOINTENSITY RESULTS

In total, 43 specimens were measured for determining the ancient field intensity. Acceptance criteria for these measurements were set as DRATS smaller than 16%, f fractions > 0.4, tail checks smaller than 10%, and standard deviation of the calculated intensity smaller than 10% absolute intensity value. Of these, only 4 were rejected. Individual specimens, and averages for each structure are presented in **table 3**.

**Table 3.** Paleointensity (Ba) results for the various samples and average for each structure. Quality factor q, f fraction (Coe 1967), and alteration checks (DRATS) are also indicated. The temperature interval is defined between minimum temperature (minT) and maximum temperature (maxT), and the paleointensity can be calculated with the number of points defined by nPI. Declination, inclination, and MAD are also given. Sample names marked with asterisks correspond to those experienced in San Diego laboratory. Ba (AARM) correspond to values obtained after applying the correction for the magnetic anisotropy.

| Sample | MinT [˚C] | MaxT [˚C] | D [˚] | I [˚] | MAD [˚] | nPi | Ba [μT] | sBa [μT] | Ba (AARM) | sBa (AARM) | q | f | Drats [%] |
|---|---|---|---|---|---|---|---|---|---|---|---|---|---|
| **Structure 1** | | | | | | | | | | | | | |
| Lv1a* | 100 | 580 | 348.9 | 61.3 | 1.9 | 15 | 62.8 | 1.6 | 64.1 | 1.6 | 41.8 | 0.94 | 5.8 |
| Lv2v* | 100 | 580 | 345.8 | 61.2 | 1.8 | 15 | 64.8 | 3.8 | 64.8 | 3.8 | 13.9 | 0.69 | 10.3 |
| Lv8z* | 100 | 540 | 358.6 | 58.5 | 1.9 | 14 | 70.7 | 2.1 | 70.3 | 2.1 | 38.7 | 0.90 | 3.9 |
| Lv8k | 150 | 520 | 354.4 | 58.9 | 2.7 | 10 | 68.8 | 2.3 | 68.8 | 4.5 | 20.8 | 0.83 | 12.9 |
| Lv10a* | 100 | 540 | 343.3 | 56.3 | 2.5 | 15 | 69.2 | 3.3 | 69.2 | 3.3 | 18.0 | 0.71 | 10.8 |
| Lv10g | 100 | 460 | 344.4 | 58.3 | 2.4 | 10 | 66.4 | 1.5 | 66.4 | 2.8 | 32.5 | 0.84 | 12.7 |
| **Mean** | | | | | | **6** | **66.5** | **2.8** | | | | | |
| **Structure 2** | | | | | | | | | | | | | |
| Lv12v | 20 | 460 | 345.7 | 59.3 | 6.4 | 11 | 67.1 | 6.4 | 67.1 | 6.4 | 5.6 | 0.48 | 6.8 |
| Lv12g* | 100 | 580 | 347.9 | 57.2 | 3.1 | 15 | 63.2 | 2.2 | 63.2 | 2.2 | 27.5 | 0.82 | 8.1 |
| Lv14g | rejected | | | | | | | | | | | | |
| Lv16a* | 100 | 580 | 350.5 | 50.4 | 2.2 | 15 | 58.5 | 2.3 | 58.5 | 2.3 | 23.9 | 0.88 | 5.6 |
| Lv20g | 20 | 430 | 348.7 | 61.0 | 9.9 | 10 | 62.9 | 2.9 | 62.9 | 2.9 | 6.4 | 0.34 | 1.6 |
| Lv23v | 20 | 400 | 4.4 | 47.6 | 4.9 | 9 | 71.0 | 3.0 | 71 | 3 | 16.2 | 0.80 | 5.7 |
| Lv23g* | 100 | 580 | 8.5 | 48.0 | 2.6 | 15 | 59.3 | 2.2 | 59.3 | 2.2 | 26.6 | 0.96 | 6.5 |
| Lv23d* | 100 | 580 | 9.3 | 48.1 | 1.5 | 15 | 60.9 | 3.0 | 60.9 | 3.0 | 18.7 | 0.93 | 4.6 |
| **Mean** | | | | | | 7 | **62.1** | **3.8** | | | | | |
| **Structure 3** | | | | | | | | | | | | | |
| Lv35a* | 150 | 580 | 355.1 | 56.9 | 1.4 | 14 | 61.6 | 0.9 | 61.6 | 0.9 | 63.5 | 0.87 | 1.3 |
| Lv35b | 20 | 430 | 353.1 | 59.2 | 3.4 | 9 | 64.2 | 3.0 | 64.2 | 3 | 30.9 | 0.92 | 7.3 |

| Sample | MinT [˚C] | MaxT [˚C] | D [˚] | I [˚] | MAD [˚] | nPi | Ba [μT] | sBa [μT] | Ba (AARM) | sBa (AARM) | q | f | Drats [%] |
|---|---|---|---|---|---|---|---|---|---|---|---|---|---|
| Lv36a | 20 | 360 | 349.1 | 56.7 | 7.3 | 6 | 67.2 | 4.0 | 67.2 | 4 | 3.4 | 0.34 | 8.9 |
| LV37a | 400 | 580 | 346.4 | 59.1 | 3.3 | 5 | 71.5 | 2.8 | 71.5 | 2.8 | 12.6 | 0.73 | 2.0 |
| Lv37e* | 100 | 580 | 349.7 | 58.5 | 1.4 | 15 | 69.9 | 1.0 | 69.0 | 1.0 | 71.3 | 0.97 | 5.6 |
| Lv38g | 20 | 580 | 350.5 | 58.4 | 2.6 | 11 | 66.9 | 1.4 | 66.88 | 1.4 | 40.7 | 0.97 | 6.0 |
| Lv38e | 100 | 620 | 351.7 | 60.9 | 2.7 | 12 | 67.2 | 1.5 | | | 33.0 | 0.92 | 15.8 |
| Lv40a* | 100 | 580 | 355.1 | 55.9 | 2.8 | 15 | 62.9 | 2.8 | 63.8 | 2.8 | 16.3 | 0.64 | 4.6 |
| Lv40b | 150 | 620 | 353.6 | 59.4 | 4.4 | 10 | 69.3 | 5.8 | 69.3 | 5.8 | 14.5 | 0.71 | 8.7 |
| LV41g* | rejected | | | | | | | | | | | | |
| Lv42b | 20 | 620 | 346.3 | 59.4 | 3.8 | 13 | 63.2 | 4.2 | 63.2 | 4.2 | 22.6 | 0.95 | 0.9 |
| Lv43b | 20 | 460 | 342.0 | 62.3 | 1.9 | 12 | 63.6 | 2.7 | 63.6 | 2.7 | 36.7 | 0.99 | 12.8 |
| Lv45a | 200 | 580 | 350.6 | 51.2 | 2.4 | 8 | 72.5 | 2.5 | 72.5 | 2.5 | 21.6 | 0.93 | 3.8 |
| Lv48a | 20 | 520 | 3.7 | 59.0 | 3 | 10 | 71.5 | 2.2 | 71.5 | 2.2 | 24.5 | 0.88 | 8.7 |
| Lv50e* | 20 | 580 | 4.4 | 56.8 | 3.6 | 16 | 80.3 | 2.4 | 80.3 | 2.4 | 26.5 | 0.87 | 12.2 |
| Lv52a* | 230 | 540 | 356.5 | 57.1 | 1.2 | 11 | 71.3 | 2.0 | 71.8 | 2.0 | 37.1 | 0.83 | 5.8 |
| Lv52e | 240 | 580 | 0.7 | 57.6 | 5 | 8 | 70.3 | 3.9 | 70.3 | 3.9 | 25.8 | 0.90 | 10.4 |
| Lv54a | 20 | 460 | 353.7 | 58.9 | 3.7 | 10 | 65.7 | 5.1 | 65.7 | 5.1 | 16.3 | 0.77 | 3.5 |
| Lv55v | rejected | | | | | | | | | | | | |
| Lv56a* | 150 | 580 | 14.7 | 58.7 | 2.3 | 14 | 72.5 | 6.5 | 72.5 | 6.5 | 10.3 | 0.98 | 11.3 |
| **Mean** | | | | | | **18** | **67.2** | **4.5** | | | | | |
| | | | | | | **Structure 4** | | | | | | | |
| Lv24a | 100 | 460 | 345.2 | 65.2 | 2.3 | 9 | 62.4 | 2.9 | 62.4 | 2.9 | 12.2 | 0.68 | 3.9 |
| Lv24e* | 100 | 580 | 343.7 | 64.2 | 1.4 | 15 | 63.7 | 2.2 | 63.7 | 2.2 | 30.0 | 0.88 | 3.2 |
| Lv26a* | 230 | 580 | 319.3 | 62.2 | 1.1 | 12 | 71.9 | 3.8 | 71.9 | 3.8 | 21.3 | 0.90 | 6.7 |
| Lv29a | 200 | 580 | 338.1 | 67.3 | 3.4 | 10 | 70.8 | 1.7 | 70.8 | 1.7 | 31.1 | 0.85 | 3.3 |
| Lv30a* | 230 | 580 | 0.9 | 65.8 | 1.7 | 12 | 72.1 | 2.6 | 72.1 | 2.6 | 29.5 | 0.84 | 2.1 |
| Lv31a* | 230 | 580 | 8.4 | 61.7 | 1.8 | 12 | 70.8 | 2.7 | 70.8 | 2.7 | 26.9 | 0.82 | 7.6 |
| Lv31g* | 230 | 580 | 7.5 | 61.5 | 1.5 | 12 | 72.5 | 2.3 | 72.5 | 2.3 | 33.6 | 0.84 | 7.8 |
| Lv31k* | rejected | | | | | | | | | | | | |
| Lv32b | 20 | 580 | 347.5 | 71.8 | 3.1 | 12 | 72.0 | 1.8 | 72 | 1.8 | 29.7 | 0.92 | 8.3 |
| **Mean** | | | | | | **9** | **69.8** | **3.5** | | | | | |

Anisotropy of the Anhysteretic Remanent Magnetization (AARM) is determined and used to minimize the influence of magnetic anisotropy on the paleointensity result. This method was introduced by Veitch et al. (1984), and it was applied to a number of specimens studied in San Diego. In our study we did not spot significant differences (see the columns Ba and Ba (AARM)). This result supports observation made by Kovacheva et al. (2009a) on similar materials.

**Figure 7** presents pairs of paleointensity determinations from Sofia and from San Diego. We always notice a good agreement between the interlaboratory comparisons.

## DISCUSSION AND CONCLUSIVE REMARKS

A summarizing **table 4** showing the average directions and intensity for each structure is presented. The second column of **table 4** gives the laboratory numbers (Sofia Lab. #, see Kovacheva et al. 2009b) attributed to these structures, and the third column gives the available independent archaeological age (Vagalinski in press a, b).

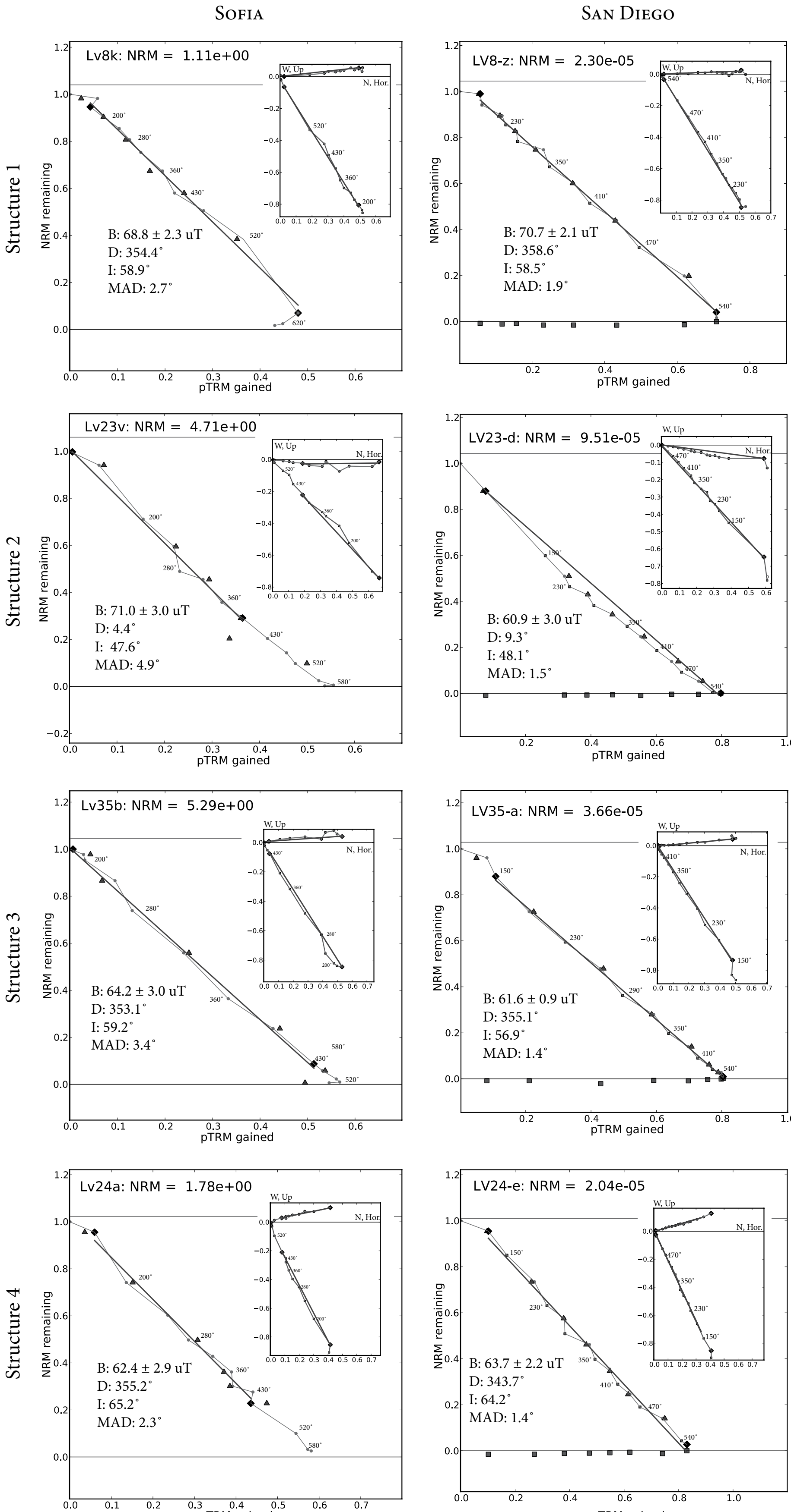


**Fig. 7**. Comparison between paleointensity experiments from Sofia (left column), and San Diego (right column). Each plot shows the Arai diagram (Arai 1963) from which the paleofield can be determined, and the Zijderveld plot showing the directions (Declinations (Inclination) as circles (squares)) in the inset.

**Table 4**. Summary of the geomagnetic field data for the four structures, together with the median archaeological age and its uncertainty.

| Structure | Sofia Lab. # | Age | σAge | n | D [˚] | I [˚] | $\alpha_{95}$ [˚] | K | nPi | Ba [μT] | σBa [μT] |
|---|---|---|---|---|---|---|---|---|---|---|---|
| 1 | 346 | 85 | 15 | 10 | 353,6 | 60,7 | 2,5 | 362,4 | 6 | 66,5 | 2,8 |
| 2 | 347 | 85 | 15 | 8 | 356,2 | 56,6 | 2,7 | 425,8 | 7 | 62,1 | 3,8 |
| 3 | 348 | 85 | 15 | 23 | 356,5 | 57,4 | 1,9 | 247,8 | 18 | 67,2 | 4,5 |
| 4 | 345 | -15 | 45 | 5 | 359,9 | 67,6 | 5,6 | 190,6 | 9 | 69,8 | 3,5 |

The agreement of the geomagnetic field values between lime kilns (structures 1 to 3) indicates that these were last used very closely in time. Structure 4 (pottery kiln) shows values that are slightly distinguishable from the other ones, and so suggests that it was used in other times. This conclusion is better seen in **figure 8**, showing the geomagnetic field variations (inclination, declination, and intensity) during the past 3000 years as based on part of the Bulgarian dataset (black closed circles, Kovacheva et al. 2009), on 3 available models (lines), and on the results of the present study (lime kilns as black empty circles and pottery kiln as an empty black star).

The Bulgarian master curves have been used successfully in past studies (Kovacheva et al. 2004; Kostadinova / Kovacheva 2008; Herries et al. 2008), and will continue to be an excellent tool for new undated archaeological sites. That is why its further refinement is a prerequisite for reliable dating.

The results presented in **figure 8** clearly indicate that a gap in the Bulgarian Master Curve of Kovacheva et al. (2009) around AD 0 is partly filled with these new, well constrained and well dated archaeomagnetic data. These new data will also provide useful constraints for regional modelling (e.g. Pavon-Carrasco et al. 2008 and 2009; Lodge / Holme 2008; Korte et al. in press).

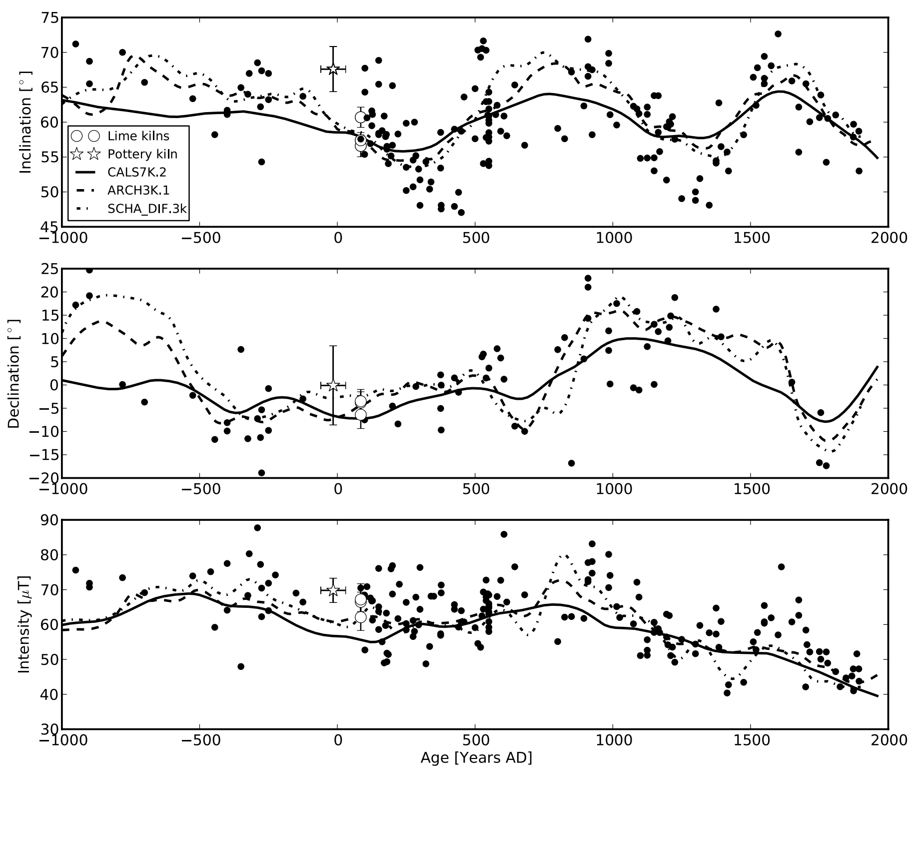


**Fig. 8**. Declination, inclination, and intensity curves of geomagnetic field during the past 3000 years. Black circles are the available Bulgarian data for this time interval, the lines are the available regional and global models (see text for details). The new measurements are given as an empty black star (pottery kiln, structure 4), and as empty black circles (lime kilns, structures 1 to 3).

This study also confirms the archaeologist assumption that all the lime kilns are from one and the same period (the directional and intensity results are very close – **fig. 8**, black empty circles). Directions from the 4th structure (the pottery kiln, black empty star) plot distinctly away from the ones of the other structures. To check this, we performed a bootstrap test for common mean (Tauxe et al. 2009) of the four structures. We used the sample averages presented in **table 2**, as well as the individual specimens' data. Results indicate that structures 2 and 3 have a common mean, but when the other structures – and in particular structure 4 – are compared this hypothesis is rejected at 95% confidence interval. This observation proves the contemporaneous use of the lime kilns from structures 2 and 3, and suggests that the pottery kiln (structure 4) was last used during another time.

**Figure 8** also shows the fit of three models (CALS7K.2, Korte / Constable 2005; ARCH3K.1, Korte et al. in press; SCHA.DIF.3k, Pavon-Carrasco et al. 2009) with the Bulgarian data. The CALS7K.2 model is a global one covering the past 7000 years, and cannot reproduce the small variations of the geomagnetic field. A better fit to the real data is achieved with the ARCH3K.1 model (Korte et al. in press), which is constructed using only archaeomagnetic data. A similar excellent fit is also produced by the SCHA.DI.00-F model (Pavon-Carrasco et al. 2008). In particular, this model is able to reproduce a minimum intensity at around AD 1400.

Although reference curves rely on independent dating of the structures (e.g., stratigraphy, archaeological context, $^{14}$C, dendrochronology), we calculated the archaeomagnetic date as comparison. We used the Lanos algorithm (Lanos 2004) to calculate the probable age of the structures using the available Bulgarian reference curves from 2002. Obtained age intervals are very similar for all structures (about 15 BC to 15 AD), they are very precise, but do not allow for further discrimination between the firing of the older Structure 4 and the more recent ones because of the existing gap in the reference curve.

Finally, we will use these new, well constrained data, together with their archaeological date for further improvements of the Bulgarian master curves.

**ACKNOWLEDGEMENT**

Fabio Donadini's work was possible with a grant by the Finnish Academy of Sciences. Reviewers are acknowledged as well.

**BIBLIOGRAPHY**

*Arai, Y.* 1963. Secular variation in intensity of the past geomagnetic field. MSc Thesis. University of Tokyo.

*Coe, R.* 1967. Paleointensities of the Earth's magnetic field determined from Tertiary and Quaternary rocks. – Journal of Geophysical Research 72, 3247-3262.

*Donadini, F. / Korte, M. / Constable, C.* 2009. Geomagnetic Field for 0-3ka: 1. New data sets for global modeling. – Geochemistry, Geophysics, Geosystems 10, Q06007.

*Dunlop, D.* 2002. Theory and application of the Day plot (Mrs/Ms versus Hcr/Hc) 1. Theoretical curves and tests using titanomagnetite data. – Journal of Geophysical Research 107, doi.: 10.1029/2001JB000486.

*Dunlop, D. / Ozdemir, O.* 1997. Rock magnetism. Fundamentals and frontiers. Cambridge Studies in Magnetism 3. Cambridge.

*Fisher, R.* 1953. Dispersion on a sphere. – Proceedings Royal Society London A 217, 295-305.

*Gomez-Paccard, M. / Chauvin, A. / Lanos, P. / Thiriot, J. / Jimenez-Castillo, P.* 2006. Archeomagnetic study of seven contemporaneous kilns from Murcia (Spain). – Physics of the Earth and Planetary Interiors 157, 16-32.

*Herries, A. / Kovacheva, M.* 2007. Using archaeomagnetism to answer archaeological questions about burnt structures at the Thracian site of Halka Bunar, Bulgaria. – Archaeologia Bulgarica 11, 3, 25-46.

*Herries, A. / Kovacheva, M. / Kostadinova, M.* 2008. Mineral magnetism and archaeomagnetic dating of a mediaeval oven from Zlatna Livada, Bulgaria. – Physics and Chemistry of the Earth 33, 496-510.

*Jordanova, N.* 1996. Rock magnetic studies in archeomagnetism and their contribution to the problem of reliable determinations of the ancient geomagnetic field intensity. PhD Thesis. Sofia University.

*Jordanova, N. / Kovacheva, M. / Hedley, I. / Kostadinova, M.* 2003. On the suitability of baked clays for archaeomagnetic studies as deduced from detailed rock-magnetic studies. – Geophysical Journal International 153, 146-158.

*Korte, M. / Mandea, M. / Matzka, J.* in press. A historical declination curve for Munich from different data sources. – Physics of the Earth and Planetary Interiors.

*Kostadinova, M. / Kovacheva, M.* 2008. Case study of the Bulgarian Neolithic archaeological site of Piperkov Chiflik and its archaeomagnetic dating. – Physics and Chemistry of the Earth 33, 511-522.

*Kovacheva, M. / Boyadziev, Y. / Kostadinova, M. / Jordanova, N. / Donadini, F. 2009a.* Updated archeomagnetic data set of the past eight millenia from the Sofia laboratory, Bulgaria. – Geochemistry, Geophysics, Geosystems 10, Q05002, doi: 10.1029/2008GC002347.

*Kovacheva, M. / Chauvin, A. / Jordanova, N. / Lanos, P. / Karloukovski, V.* 2009b. Remanence anisotropy effect on the palaeointensity results obtained from various archaeological materials, excluding pottery. – Earth, Planets, and Space 61, 711-732.

*Kovacheva, M. / Hedley, I. / Jorvanova, N. / Kostadinova, M. / Gigov, V.* 2004. Archaeomagnetic dating of archaeological sites from Switzerland and Bulgaria. – Journal of Archeological Science 31, 1463-1479.

*Kovacheva, M. / Jordanova, N. / Karloukovski, V.* 1998. Geomagnetic field variations as determined from Bulgarian archaeomagnetic data. Part II: the last 8000 years. – Surveys in Geophysics 19, 431-460.

*Lanos, P.* 2004. Bayesian inference of calibration curves: application to archaeomagnetism. In: Buck, C. / Millard, A. (eds.). Tools for constructing chronologies, crossing disciplinary boundaries. Volume 177, Lecture Notes in Statistics. London, 43-82.

*Lanos, P. / LeGoff, M. / Kovacheva, M. / Schnepp, E.* 2005. Hierarchical modelling of archaeomagnetic data and curve estimation by moving average technique. – Geophysical Journal International 160, 440-476.

*Le-Goff, M. / Gallet, Y. / Genevey, A. / Warme, N.* 2002. On archeomagnetic secular variation curves and archeomagnetic dating. – Physics of the Earth and Planetary Interiors 134, 203-211.

*Lodge, A. / Holme, R.* 2008. Towards a new approach to archeomagnetic dating in Europe using geomagnetic field modeling. – Archaeometry 50, 309-322.

*Lowrie, W.* 1990. Identification of ferromagnetic minerals in a rock by coercivity and unblocking temperature properties. – Geophysical Research Letters 2, 159-162.

*Lowrie, W. / Fuller, M.* 1971. On the alternating field characteristics of multidomain thermoremanent magnetization in magnetite. – Journal of Geophysical Research 76, 6339-6349.

*Marton, P.* 2010. Two thousand years of geomagnetic old direction over central Europe revealed by indirect measurements. – Geophysical Journal International 181, 261-268.

*McIntosh, G. / Kovacheva, M. / Osete, M.L. / Casas, L.* 2007. Widespread occurrence of a novel high coercivity, thermally stable, low unblocking temperature magnetic phase in heated archeological material. – Geophysical Research Letters 34, L21302.

*Merrill, R. / McElhinny, M. / McFadden, M.* 1996. The magnetic field of the Earth. San Diego.

*Pavon-Carrasco, F.J. / Osete, M.L. / Torta, J.M. / Gaya-Piqué, L.R.* 2009. A regional archeomagnetic model for Europe for the last 3000 years, SCHA. DIF.3K: Applications to archeomagnetic dating. – Geochemistry, Geophysics, Geosystems 10, Q03013, doi: 10.1029/2008GC002244.

*Pavon-Carrasco, F.J. / Osete, M.L. / Torta, J.M. / Gaya-Piqué, L.R.* 2008. A Regional Archaeomagnetic Model for the Palaeointensity in Europe for the last 2000 Years and its Implications for Climatic Change. – Pure and Applied Geophysics 165, 1209-1225.

*Riisager, P. / Riisager, J.* 2001. Detecting multidomain magnetic grains in Thellier paleointensity experiments. – Physics of the Earth and Planetary Interiors 125, 111-117.

*Schnepp, E. / Lanos, P.* 2006. A preliminary secular variation reference curve for archaeomagnetic dating in Austria. – Geophysical Journal International 166, 91-96.

*Tauxe, L. / Butler, R. / Banerjee, S. / Van der Voo, R.* 2009. Essentials of Paleomagnetism. San Diego.

*Tauxe, L. / Staudigel, H.* 2004. Strength of the geomagnetic field in the Cretaceous Normal Superchron: New data from submarine basaltic glass of the Troodos Ophiolite. – Geochemistry, Geophysics, Geosystems 5, Q02H06.

*Tema, E. / Hedley, I. / Lanos, P.* 2006. Archaeomagnetism in Italy: a compilation of data including new results and a preliminary Italian secular variation curve. – Geophysical Journal International 167, 1160-1171.

*Vagalinski, L.* in press, a. Light industry in Roman Thrace: The case of the lime production. In: Haynes, I. (ed.). Early Roman Thrace. Journal of Roman Archaeology, Supplementary Series.

*Vagalinski, L.* in press, b. A new late La Tene pottery kiln on the Lower Danube (North Bulgaria). In: Jevtič, M. / M. Guštin (eds.). The Eastern Celts between Hellenistic and Roman world. International Archaeological Symposium, Serbia, Vršac 1.-4.11.2007.

*Veitch, R.-J. / Hedley, I.-G. / Wagner, J.-J.* 1984. An investigation of the intensity of the geomagnetic field during Roman times using magnetically anisotropic bricks and tiles. – Archives des Sciences Genève 37, 359-373.

*Wessel, P. / Smith, W.* 1991. Free software helps map and display data. – Eos Trans. AGU 72, 441.

# Археомагнитно изследване на римски пещи за вар (1 в. сл. Хр.) и една керамична пещ (1 в. пр. Хр. – 1 в. сл. Хр.) край село Кривина, България, като принос към археомагнитното датиране

**Фабио ДОНАДИНИ / Мери КОВАЧЕВА / Мария КОСТАДИНОВА-АВРАМОВА**

**(резюме)**

Статията представя детайлни археомагнитни изследвания на останките от 7 пещи за вар и една керамична пещ, разкрити край село Кривина, Русенско, на брега на р. Дунав в Североизточна България. Тези пещи са групирани в 4 структури според тяхното пространствено разположение и се отнасят към началото на нашата ера. Колекцията образци показаха благоприятни магнитни свойства, осигуряващи достоверни археомагнитни измервания. В тази работа ние изследвахме едновременно посоката (деклинация D и инклинация I) и интензитета (Ba) на геомагнитното поле, отнасящи се за времето и мястото на последното опалване на пещите. Тези резултати ще бъдат използвани като референтни точки за подобряване на българските палеовекови археомагнитни криви, както и за глобалните и регионални модели на геомагнитното поле, които могат също да се използват за датиране в археологията.

Част от колекцията бе изследвана в Скрипс Институт по Океанография в Сан Диего, а част в Палеомагнитната лаборатория на Геофизичен Институт на БАН (София). Изключителното съответствие между тези независими измервания показва високото качество на материала и валидността на приложените методи.

Резултатите са обобщени като средни по структури, които представят различните пещи. Първа до трета структура се предполагат едновременни и имат резултати: D: 353.6˚, I: 60.7˚, Ba: 67.2 μT (1-ва структура), D: 356.2˚, I: 56.6˚, Ba: 63.2 μT (2-ра структура), D: 356.5˚, I: 57.4˚, Ba: 67.9 μT (3-та структура). 4-та структура е по-стара по археологически данни и даде: D: 359.9˚, I: 67.6˚, Ba: 69.0 μT. Статистическите тестове за сравнение на осреднените посоки на четирите структури също отхвърлят хипотезата за общо средно между 4-та структура и останалите на 95% доверително ниво. Това показва, че времето, когато 4-тата структура (керамичната пещ) е използвана за последен път, се различава от времето на последното опалване на останалите структури.

Тези нови резултати попълват частично една от празнотите в българските референтни криви (150 г. пр. Хр. – 85 г. сл. Хр.) и показват, че подобрение по отношение на моделирането на вариациите на геомагнитното поле в миналото може да се постигне с археомагнитно изследване на нови, добре датирани колекции.

**Dr. Fabio Donadini**
Institut für Geophysik
ETH Zürich
Sonneggstrasse 5
CH-8092 Zürich
fabio.donadini@gmail.com

**Prof. DSc Mary Kovacheva**
Palaeomagnetic laboratory of the Geophysical Institute
Bulgarian Academy of Sciences
BG-1113 Sofia
marykov@abv.bg

**Dr. Maria Kostadinova-Avramova**
Palaeomagnetic laboratory of the Geophysical Institute
Bulgarian Academy of Sciences
BG-1113 Sofia
miki4740@abv.bg